Proc. Natl. Acad. Sci. USA
Vol. 74, No. 5, pp. 1789–1793, May 1977
Chemistry

Energy-structure correlation in metalloporphyrins and the control of oxygen binding by hemoglobin

(allosteric interactions/energy functions/spin state/heme vibration)

ARIEH WARSHEL

Department of Chemistry, University of Southern California, Los Angeles, California 90007; and MRC Laboratory of Molecular Biology, Hills Road, Cambridge CB2 2QH, England

Communicated by Max F. Perutz, March 7, 1977

ABSTRACT **The contribution of the porphyrin skeleton to the potential energy surface of metalloporphyrins is calculated by the semiempirical method of quantum mechanical extension of the consistent force field to π electron molecules. This calculation makes it possible to correlate the observed structure of metalloporphyrins with the strain energy of the porphyrin skeleton. It is found that the out-of-plane metal displacement in pentacoordinate heme systems is due to both the restricted size of the porphyrin hole and the "1–3" steric interaction between the axial ligand and the heme nitrogens. The main components of the active site of hemoglobin are simulated by a histidine-heme-oxygen system. The energy surface of this system provides a quantitative explanation for the control of ligand binding by hemoglobin. It is shown that the heme acts as a diaphragm, designed to provide simultaneous binding to the histidine and the sixth ligand under the steric requirements of the 1–3 interactions. The dependence of the hemoglobin potential surface on the distance between the proximal histidine and the heme plane is evaluated for the R and T states, using the calculated heme potential and the observed energy of heme–heme interaction.**

X-ray and biochemical experiments have provided detailed information about the structure of hemoglobin and its biological functions (for a recent review see ref. 1). Many studies have been concerned with the analysis of the molecular origin of the heme–heme interaction (the increase in the affinity of the fourth bound oxygen relative to that of the first bound oxygen). Perutz and coworkers (2–5) compared the structures of the high and low oxygen affinity states of hemoglobin. They suggested that in the low oxygen affinity state the protein pulls the iron away from the heme plane, and opposes the transition to the low spin state which is needed for combination with oxygen. Hopfield (6) used a simple model of two springs to suggest that the heme–heme interaction energy is distributed among many degrees of freedom in the protein and not in the relatively rigid heme. Experiments (7, 8) have not found evidence for significant strain in the heme group.

At the present time, despite the above studies, the role of the active site of hemoglobin in the control of oxygen binding is not fully understood. For example, the reasons for the change in heme geometry upon binding of oxygen and the relation between the heme tension, spin state, and oxygen affinity are still unclear. It is also questionable whether or not the heme group can be considered a rigid system. The analysis of these problems requires information about the energy surface of the heme group and such information cannot be obtained directly from structural or spectroscopic studies.

This work uses energy calculations to study the correlation between the energy and structure of the active site system shown in Fig. 1. These quantitative calculations make it possible to examine the molecular basis for the control of oxygen binding by hemoglobin. It is found that the main reason for the change in heme geometry upon binding of oxygen is the "1–3" steric interaction (see Fig. 1) between the oxygen and the heme nitrogens. Because of the effect of the 1–3 interactions the heme acts as a diaphragm designed to provide simultaneous binding to two groups that cannot approach too closely to the center of the diaphragm base. The hemoglobin molecule uses this arrangement to regulate the oxygen affinity (see Fig. 5).

Abbreviations: TPP, tetraphenyl porphyrin; MeIm, methyl imidazole; NMR, nuclear magnetic resonance; SCF, self-consistent field, QCFF/PI, quantum mechanical extension of the consistent force field method to π electron molecules.

Correlation between heme energy and metal size

In recent years, the stereochemistry of porphyrins and metalloporphyrins has been studied extensively (for a review see ref. 9). These studies indicate that when the metal size increases, the metal is displaced out of the porphyrin plane because it cannot fit into the porphyrin hole. Unfortunately, the observed out-of-plane displacement of the metal cannot give direct information about the detailed energy balance in the heme system and about the "strain" energy of different deformations.

One way to analyze the correlation between the structure and energy of the heme group is to use a reliable theoretical scheme that can be calibrated to fit experimental data. This is done here by the QCFF/PI method (10–13) in which the σ electron energy surface is described by empirical potential functions and the π electron energy surface is described by a semiempirical quantum mechanical treatment. For the case of metalloporphyrins, the quantum mechanical treatment is extended to include (in addition to the π heme orbitals) the d_{z^2}, d_{xy}, d_{xz}, d_{yz}, $d_{x^2-y^2}$, and 4*s* orbitals of the metal, the lone pairs of the heme nitrogens, and the lone pairs of the axial ligands. The heme potential used here is based on extensive fitting of the QCFF/PI parameters to many independent properties of conjugated hydrocarbons and nitrogen-containing molecules (12). This potential gives good agreement between the calculated and observed equilibrium geometries and vibrational frequencies of the heme group for different sizes of its core (14).

The strain in the porphyrin skeleton is analyzed as a function of the metal size by using the adiabatic mapping procedure (10–13, 15). In this procedure, using b_0 to simulate the metal size, an external constraint $V' = \Sigma_{i=1}^{4} K(b_i - b_o)^2$ is introduced for the four metal–nitrogen bonds (b_i). The energy of the heme and the constraint (excluding the quantum mechanical energy of interaction between the metal orbitals and the porphyrin) is minimized *with respect to all atomic coordinates* for selected values of b_o. Obviously at some stage the metal is displaced out of the heme plane. The out-of-plane displacement is monitored by introducing a second adiabatic constraint for the displacement (z') of the metal from the mean nitrogen plane. Fig. 2 shows these adiabatic energy curves as a function of the distance (z) between the metal and the mean heme plane for different

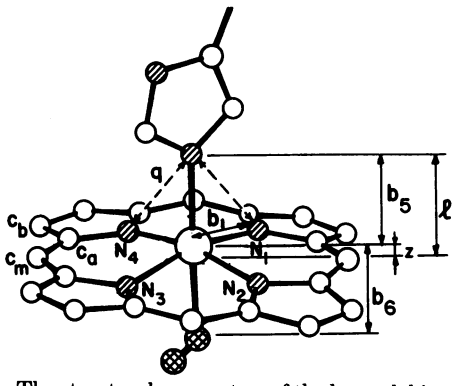

FIG. 1. The structural parameters of the hemoglobin active site. b_1, b_5, and b_6 are the bonds from the iron atom to the porphyrin nitrogens, the proximal histidine, and the oxygen, respectively. q is a 1–3 distance, z is the displacement of the iron from the mean heme plane, and l is the distance between the proximal histidine nitrogen and the mean heme plane.

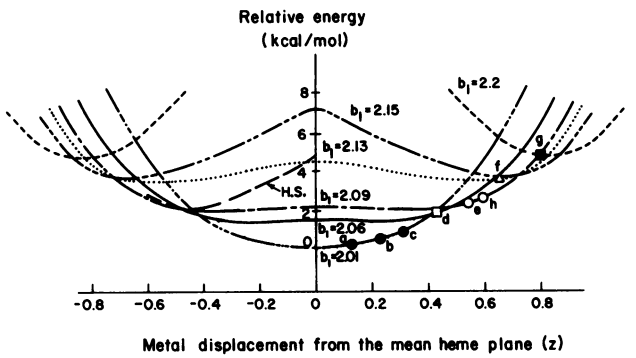

FIG. 2. Calculated adiabatic potential surface V_s for the deformation of the porphyrin skeleton. V_s is given as a function of the metal displacement from the mean heme plane (z) for given metal-nitrogen distances (b_1). The H.S. curve gives the sum of V_s, $V_{z'}$, and V_{1-3} for a high spin pentacoordinate system with b_1 = 2.09 Å. The observed points (from the references mentioned in ref. 9) are placed on the corresponding b_1 and z values and designated by ●, □, ○, △, and ■ for b_1 values 2.01, 2.06, 2.09, 2.13, and 2.2 Å, respectively. The following observed points are included: (a) (1-MeIm)Co(TPP); (b) (ON)Fe(TPP); (c) (Cl)Mn(TPP); (d) (ClO_4)Zn(TPP); (e) (2-MeIm)-Fe(TPP); (f) (1-MeIm)Mn(TPP); (g) (Cl)Tl(OEP); (h) deoxyhemoglobin (16).

values of the metal-nitrogen distance (b_1), which is almost equal to b_o. Note how the minima of the curves are shifted to $z > 0$ when the metal size increases.* A check on the calculated potential surface was obtained by the analysis of the heme expansion vibration at about 360 cm^{-1}. This analysis gave a potential of the form $v_s = 160(b_1 - 2.01)^2$ kcal/mol (14) for the expansion of the porphyrin skeleton (s designates skeleton). This experimental potential is in good agreement with the calculated dependence of the heme energy on b_1, for $z = 0$.

Fig. 2 provides a useful correlation between the energy and structure of metalloporphyrins. That is, one can analyze the energy of heme deformation of the molecule under study by locating the observed out-of-plane deformation (z_{obs}) along the $b_1 = b_{obs}$ calculated curve. When z_{obs} is not at the minimum of the $b_1 = b_{obs}$ curve, then the energy difference $V(z_{obs},b_{obs}) - V(z_{min},b_{obs})$ indicates extra strain that is not due to the metal size. For example, point c in Fig. 2 implies that in (Cl)-Mn(TPP) the out-of-plane deformation is due to strain of about 0.8 kcal/mol which does not result from the metal size. Since Fig. 2 gives only the pure porphyrin contribution, the extra strain energy can be due to the 1–3 steric interaction (V_{1-3}) between the fifth ligand and the heme nitrogens, and/or the energy of interaction between the metal orbitals and the orbitals of the heme nitrogen. These contributions were analyzed in the following manner:† (*i*) The stretching energy of the Fe–N bonds is approximated by $V_b = \Sigma_{i=1}^{4} 70\,(b_i - \bar{b}_0)^2$ kcal/mol where the force constant is obtained from vibrational analysis of $M(CO)_4$ systems and from analysis of the heme expansion vibration. $\bar{b}_o$ is determined as 1.94 Å for low spin Fe-porphyrins by fitting the calculated and observed geometries of molecules with different hole radii [i.e., Fe(TPP), H_2(TPP), Co(TPP), and vitamin B_{12}]. A value of 2.06 Å is obtained for the $\bar{b}_0$ of the high spin Fe-porphyrin by taking the empirical difference between low spin and high spin bonds as 0.12 Å. (*ii*) The energy of displacement of the low spin metal from the mean nitrogen plane is approximated by $V_{z'} = 25(z')^2$ kcal/mol, where the force constant is obtained by analyzing vibrations of $M(CN^-)_4$ and $M(CO)_4$ systems (17). In order to analyze the high spin pentacoordinate case, I calibrate the SCF (open shell) quantum mechanical calculations by fitting the calculated and observed $V_{z'}$ for the low spin state. The calibrated parameters give $V_{z'} = 8(z')^2$ for the high spin state. (*iii*) The 1–3 steric interaction is described by a potential function of the form $V_{1-3} = \epsilon \exp\{-\mu(q - q_o)\}$ where q is the 1–3 distance. The interaction between two nitrogen atoms is obtained by fixing q_o at the average observed value (2.92 Å), evaluating μ = 2.5 $Å^{-1}$ from the functional dependence of the nitrogen-nitrogen overlap integrals, and evaluating ϵ = 1.3 kcal/mol by fitting the calculated and observed differences between b_1 of Fe(TPP) and b_1 of $(PiP)_2$-Fe(TPP) [where the difference in b_1 is attributed to the balance between the 1–3 interaction potential and the expansion potential ($V_s + V_b$)]. This result is confirmed by finding that the out-of-plane displacement of low spin (ON)Fe(TPP) corresponds to the equilibrium between the V_{1-3} potential and the out-of-plane potential ($V_{z'}$) of the low spin state. The interaction between oxygen and nitrogen is estimated by using the same value for ϵ as in the N···N case, and a value of 2.62 Å for q_o from the corresponding difference between the N and O van der Waals radii (12).

The total heme potential V_H is composed of the pure porphyrin skeleton deformation energy (V_s) and the sum of V_b, V_z, and V_{1-3}. Fig. 2 shows that for a high spin system with $b_1 \sim 2.09$ Å and $z \sim 0.5$ Å the extra strain (due to V_{1-3} and $V_{z'}$) is small. Thus, a large part of the out-of-plane displacement can be accounted for by the fact that the metal size is larger than the size of the hole of the planar porphyrin. However, the 1–3 steric interaction (see the H.S. curve in Fig. 2) is also important in stabilizing high spin systems in the nonplanar geometries.

Potential surface of hemoglobin active site

The quaternary structure of hemoglobin is characterized by two states, R (relaxed) and T (tense), with low and high ligand affinity, respectively (2, 3). The average tertiary structures of the α and β subunits in the R and T states are designated here as r and t, respectively. In order to understand the control of the oxygen affinity one may consider the energies and struc-

* The calculated hole radius of the hypothetical "strainless" porphyrin (K = 0 in the V' constraint) is calibrated by the difference between the calculated and observed geometries of H_2(TPP). This yields a "strainless" hole radius of 2.01 ± 0.01 Å.

† Rather than attempting to determine these contributions by pure quantum mechanical calculations, I prefer to use a semiempirical approach calibrated by experimental information. This reflects a belief that the present quantum mechanical calculation scheme can only give a general trend for the potential surface of metalloporphyrins and not quantitative results. On the other hand, there is now sufficient experimental information, on related systems, to make it possible to achieve an unambiguous calibration of the semiempirical parameters.

Table 1. Structural parameters of the hemoglobin active site[a]

State	z	b_5	$l = b_5 + z$	b_1	b_6
$t^{(d)}$	0.61[b]	2.16[c]	l_t^d = 2.77	2.09[c]	—
$r^{(o)}$	0.0[d]	2.07[e]	l_r^o = 2.07	2.00[e]	1.76[e]
$r^{(d)}$	0.55[f]	2.16[c,f]	l_r^d = 2.71	2.09[f]	—
$t^{(o)}$	0.03[g]	2.11[g]	l_t^o = 2.14	2.00[h]	1.78[g]

[a] Length in Å.
[b] Deoxyhemoglobin (16) (average of α and β subunits).
[c] (1-MeIm)Fe(TPP) and (2-MeIm)Fe(TPP) (9).
[d] Ref. 18.
[e] Picket-fence porphyrin (9).
[f] The value of z_r^d = 0.55 Å is taken from ref. 19. The observation of small change in z is supported by resonance Raman experiments (20) that show that the spin state marker frequencies (21) [which are very sensitive to the heme expansion (14, 22)] are the same in both $r^{(d)}$ and $t^{(d)}$. Thus, b_1 is still approximately 2.08 Å, and therefore z must still be large.
[g] Estimated from the present work.
[h] The low spin b_1 must be similar to b_1 in $r^{(o)}$.

tures of the $t^{(d)}$, $r^{(d)}$, $t^{(o)}$, and $r^{(o)}$ states which designate, respectively, the t and r structures in the unbound (deoxy) and bound (oxy) sixth ligand states. The structural information for the different states is summarized in Table 1.

The heme–heme interaction (denoted here as $\Delta\bar{G}$) is the difference in oxygen affinity between the r and t states. This energy difference can be evaluated by extending the calculations of the previous section to the complete active site system. The potential surface of the active site is evaluated by considering the heme potential (V_H) and the bonding potential of the axial ligands. The heme potential is described in the previous section. The bonding potential of the axial ligands can be represented by a Morse type potential $M(b) = D[\exp\{-2\bar{a}(b - b_o)\} - 2\exp\{-\bar{a}(b - b_o)\}]$. The dissociation energies D are taken as 17 and 16 kcal/mol for iron-histidine (23, 24) and iron-oxygen (25) bonds respectively.‡ A value of 2.4 Å^{-1} is estimated for the parameter $\bar{a}$ by analyzing the stretching vibrations of transition metal complexes (17). The equilibrium parameters b_o are taken as the corresponding observed equilibrium values (Table 1).

The general form of the energy of the oxy state can be approximated by:

$$E^o \simeq V_H{}^o(z) + M_5{}^o(b_5) + M_6{}^o(b_6) + E_p(l) \quad [1]$$

in which V_H is the energy of the heme system, $M_5(b_5)$ and $M_6(b_6)$ are the Morse potentials for the b_5 and b_6 bonds, respectively, and E_p is the protein free energy which depends here only on the distance l. An analogous expression is used for E^d.

Eq. 1 becomes more meaningful if it is expressed in terms of the least energy path for the distance l. The energy of the active site system along this path can be expressed as:

$$E_A(l) = V_H[z(l)] + M_5[b_5(l)] + M_6[b_6(l)] \quad [2]$$

in which A designates active site, whereas $z(l)$, $b_5(l)$ and $b_6(l)$ indicate explicitly the least energy path of the corresponding variables. The calculated potential E_A for the oxy and deoxy states is presented in Fig. 3. The oxy potential is much steeper than the deoxy one in the $z > 0$ region because the out-of-plane motion toward the fifth ligand is hindered by the 1–3 steric interaction between the heme nitrogens and the sixth ligand.

‡ The change in D between low spin and high spin cases is included here in the difference between the corresponding V_H.

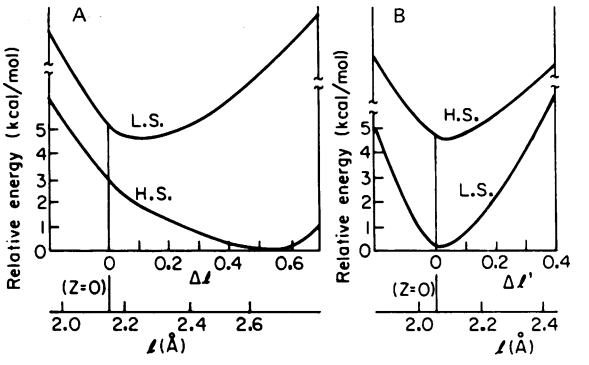

FIG. 3. (*A*) The heme-histidine potential surface along the least energy path of l in the high spin deoxy state. Δl designates $l - \bar{b}_5$ (where $\bar{b}_5$ is the unstrained length of b_5). H.S. and L.S. are, respectively, the high spin (b_1 = 2.09 Å) and low spin (b_1 = 2.01 Å) potential surfaces. The relative energy of the two spin states is arbitrary because the calculation of the energy of change in spin state is not sufficiently accurate. (*B*) The heme-histidine-oxygen potential surface along the least energy path of l in the oxy state. The notation is the same as in *A* except that $\Delta l_5' = l_5 - \bar{b}_5'$.

With this least energy potential one can write (for example) the energy of the $E_t{}^o$ state as:

$$E_t{}^o = E_A{}^o(l_t{}^o) + E_p{}^t(l_t{}^o) \quad [3]$$

The energy of the other three states can be expressed analogously. The oxygen binding energy is now given by:

$$\Delta E_r{}^{d\to o} = (E_r{}^o - E_r{}^d) = [E_A{}^o(l_r{}^o) - E_A{}^d(l_r{}^d)] + [E_p{}^r(l_r{}^o) - E_p{}^r(l_r{}^d)]$$

$$\Delta E_t{}^{d\to o} = (E_t{}^o - E_t{}^d) = [E_A{}^o(l_t{}^o) - E_A{}^d(l_t{}^d)] + [E_p{}^t(l_t{}^o) - E_p{}^t(l_t{}^d)] \quad [4]$$

The heme–heme interaction $\Delta\bar{G}$ is the difference in oxygen affinity between the r and t states and is given by:

$$\Delta\bar{G} = [E_A{}^o(l_t{}^o) - E_A{}^o(l_r{}^o)] - [E_A{}^d(l_t{}^d) - E_A{}^d(l_r{}^d)] + [E_p{}^t(l_t{}^o) - E_p{}^t(l_t{}^d)] - [E_p{}^r(l_r{}^o) - E_p{}^r(l_r{}^d)] \quad [5]$$

This equation can be rewritten as:

$$\Delta\bar{G} = (\Delta E_A{}^o)^{r\to t} - (\Delta E_A{}^d)^{r\to t} + (\Delta E_p{}^t)^{d\to o} - (\Delta E_p{}^r)^{d\to o} \quad [6]$$

in which all the contributions are positive.

To analyze the factors which determine the heme–heme

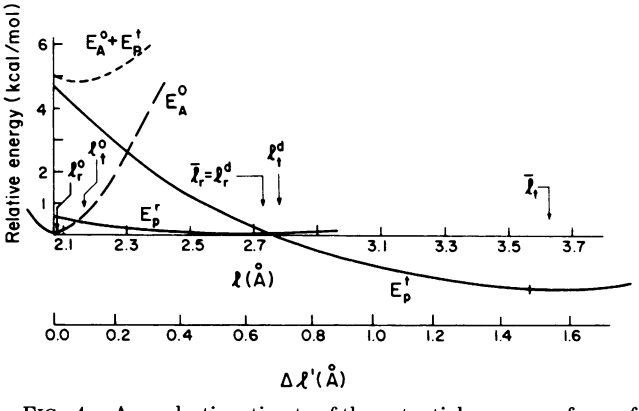

FIG. 4. A quadratic estimate of the potential energy surfaces of the $E_p{}^t$ and $E_p{}^r$ states. $\bar{l}_r$ and $\bar{l}_t$ are the equilibrium values of l in the $E_p{}^r$ and $E_p{}^t$ energy surfaces, respectively. The figure also presents the $E_A{}^0$ energy surfaces and the sum $E_A{}^o + E_p{}^t$ which gives a minimum at $l_t{}^o$.

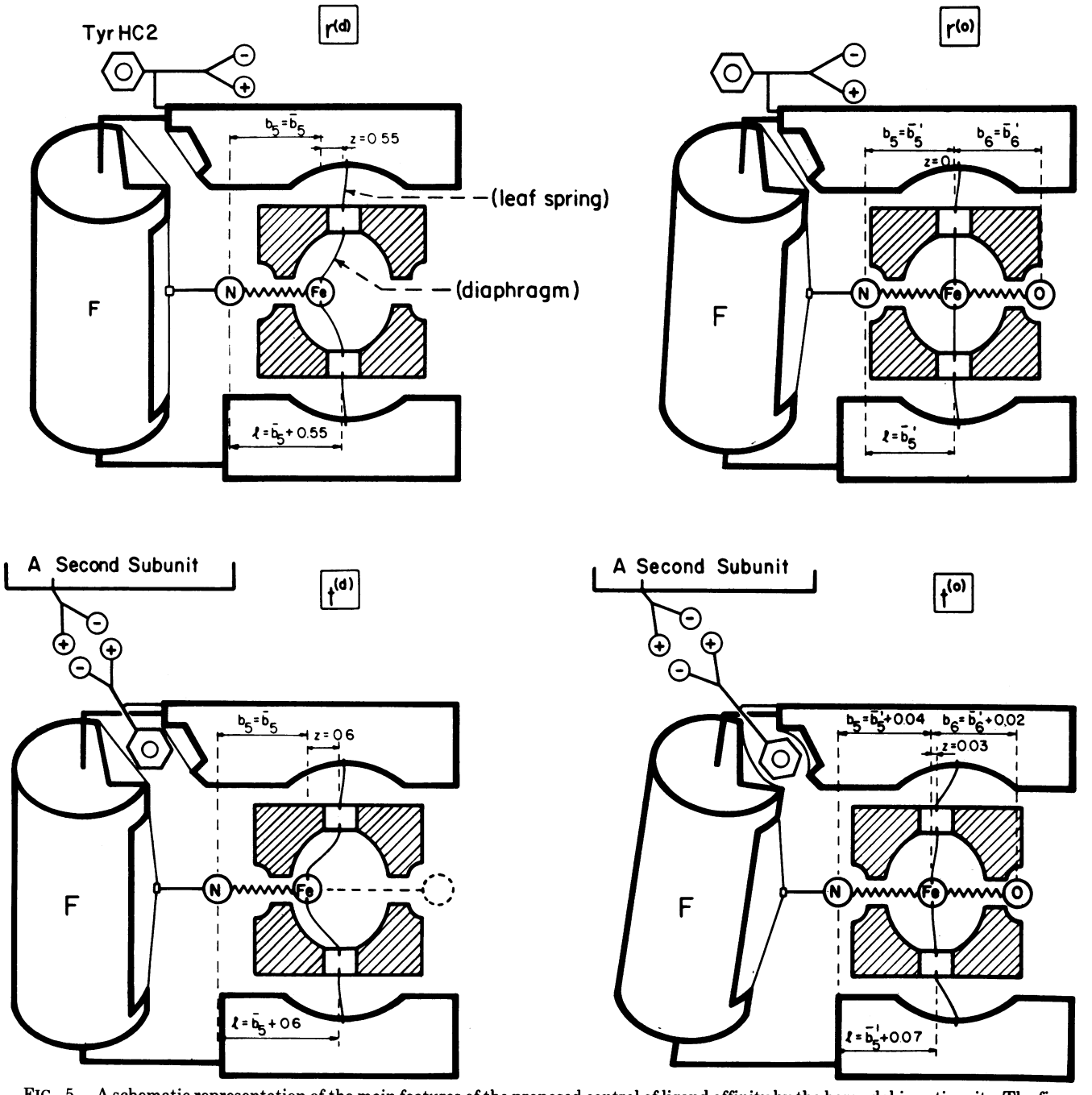

FIG. 5. A schematic representation of the main features of the proposed control of ligand affinity by the hemoglobin active site. The figure compares two states, with ligand (o) and without ligand (d), both in the t and r tertiary structures. Views are shown of cross sections taken perpendicular to the heme plane. The solid line through the Fe atom represents the edge-on projection of the heme (diaphragm). The crossed-hatched areas represent the regions restricted by the 1–3 steric interaction [i.e., q (see Fig. 1) cannot be smaller than q_o]. An incoming ligand is presented (dashed line) in the figure of the $t^{(d)}$ state. In this case, the 1–3 interaction hinders the formation of a strong b_6 bond as long as the iron is in the $z > 0$ region. The proximal histidine nitrogen is connected to the F helix. The effect of the change in the quaternary structure is represented here only by the coupling of the motion of tyrosine HC2 with the formation of the corresponding salt bridge. The strain of the protein in the $t^{(o)}$ state is represented at three leaf springs: the tyrosine pocket, the F helix, and the noncovalent bonds to the heme.

interaction, I estimate the different terms in Eq. 6. $\Delta E_A{}^d$ is estimated from Fig. 3 as 0.3 kcal/mol. A rough estimate of $\Delta E_p{}^r = 0.6$ kcal/mol is obtained by comparing the free energy of oxygen binding of picket-fence porphyrin, myoglobin, and hemoglobin (25). By using the estimate of $\Delta E_p{}^r = 0.6$ kcal/mol, the calculated $E_A{}^o$, the calculated $E_A{}^d$, and the observed $\Delta\bar{G}$ [3.6 kcal/mol (1)], one obtains quadratic approximations of the forms $E_p{}^r \sim 1.5\,(l - \bar{l}_r)^2$ kcal/mol and $E_p{}^t \sim 2.8(l - \bar{l}_t)^2$, where $\bar{l}_r$ is set equal to $l_r{}^d$ and the best $\bar{l}_t$ is found to be ~3.63 Å. These potentials give $l_t{}^o - l_r{}^o = 0.075$ Å, $\Delta E_p{}^t = 4.0$ kcal/mol, and $\Delta E_A{}^o = 0.5$ kcal/mol. The quadratic estimates of $E_p{}^t$ and $E_p{}^r$ are drawn in Fig. 4.

Control of ligand binding by hemoglobin

As shown in the previous section, the main feature of the active site potential surface is the change from a rather shallow potential (with a minimum at $z \sim 0.6$ Å) in the deoxy state to a much steeper potential (with a minimum at $z \sim 0$) in the oxy state. This change is mainly due to the 1–3 steric interactions. In view of this result, I suggest that the active site of hemoglobin

controls the oxygen binding according to the model presented in Fig. 5. The active site in this model is composed of a diaphragm (the heme) which can provide simultaneous binding to two systems, the protein (via the proximal histidine) and the oxygen. The approach of the oxygen and the histidine to the center of the diaphragm base is limited by the 1–3 steric interactions. The model is best described by following the process of oxygen binding: In the R quaternary structure the interaction between the subunits is small, and $E_p(l)$ has a minimum at ~2.7 Å. In the T quaternary structure, the interaction between the subunits shifts the minimum to ~3.6 Å. This change in structure does not lead to large strain in the heme-protein bond because the $t^{(d)}$ position of the iron corresponds to the shallow region of the $E_p{}^t$ potential. When the first oxygen approaches the $t^{(d)}$ heme in the T state it cannot form a strong bond as the iron is on the opposite side of the heme plane. The iron can be displaced toward the oxygen but this motion pulls the histidine and eventually reduces the distance between the heme plane and the F helix, transferring the strain to the protein. Thus, instead of getting the full oxygen binding energy the T state pays for straining the protein, and to some extent b_5 and b_6. The strain in the $t^{(o)}$ subunits becomes smaller if the tyrosine is expelled from its pocket and if the salt bridges between the subunits are broken. After binding of three oxygens, the strain in the $t^{(o)}$ subunits becomes sufficient to shift the system to the R quaternary structure (all the subunits being disconnected). Now the fourth subunit is in the $r^{(o)}$ state. The oxygen affinity in $r^{(o)}$ is 3.6 kcal/mol larger than in $t^{(d)}$ because the oxygen binding leads to smaller strain in the protein.

The present calculation uses a realistic molecular model for the active site of hemoglobin with the following conclusions: (*i*) The heme–heme interaction is mainly localized in the protein (in agreement with Hopfield's qualitative model) although approximately 15% of this energy is stored in the heme. (*ii*) The hemoglobin potential surface can be as steep as the heme potential surface (in contrast to the assumption in ref. 6), but the protein is built in such a way that the $t^{(d)}$ and $r^{(d)}$ states are in the shallow region of its potential. (*iii*) The change in spin state should be considered more a consequence of ligand binding than the major factor in the control of oxygen affinity. In fact, because both $r^{(o)}$ and $t^{(o)}$ are low spin states while $t^{(d)}$ and $r^{(d)}$ are high spin states the heme–heme interaction does not involve the energy of changing spin states.§ Thus, although Perutz's model of reciprocal relation between the protein tension and the oxygen affinity is correct, it is better to emphasize the change in heme geometry rather than the change in spin state. That is, the heme simply provides a relatively rigid system that *must* change geometry upon ligand binding to give simultaneous binding for the histidine and the oxygen under the constraint of the 1–3 steric interaction.

§ Whereas Eq. 4 includes implicitly the energy of changing the spin state, Eq. 5 includes only the change of energy between two geometries with the same spin state.

I thank Drs. M. Perutz, M. Kamen, T. Takano, R. Noble, and C. Connel for stimulating discussions. This work was supported by the European Molecular Biology Organization and by the Chemical-Biological Development Laboratory at the University of Southern California.

The costs of publication of this article were defrayed in part by the payment of page charges from funds made available to support the research which is the subject of the article. This article must therefore be hereby marked "advertisement" in accordance with 18 U. S. C. §1734 solely to indicate this fact.

1. Baldwin, J. M. (1975) *Prog. Biophys. Mol. Biol.* **29,** 225–320.
2. Perutz, M. F. (1970) *Nature* **228,** 726–734.
3. Perutz, M. F. (1972) *Nature* **237,** 495–499.
4. Perutz, M. F., Ladner, J. E., Simon, S. R. & Ho, C. (1974) *Biochemistry* **13,** 2163–2173.
5. Perutz, M. F., Heidner, E. J., Ladner, J. E., Beetlestone, J. G., Ho, C. & Slad, E. F. (1974) *Biochemistry* **13,** 2187–2200.
6. Hopfield, J. J. (1973) *J. Mol. Biol.* **77,** 207–222.
7. Ogawa, S. & Shulman, R. G. (1972) *J. Mol. Biol.* **70,** 315–336.
8. Eisenberger, P., Shulman, R. G., Brown, G. S. & Ogawa, S. (1976) *Proc. Natl. Acad. Sci. USA* **73,** 491–495.
9. Hoard, J. L. (1975) in *Porphyrins and Metalloporphyrins,* ed. Kevin, M. S. (Elsevier Publishing Co., Amsterdam), pp. 317–379.
10. Warshel, A. & Karplus, M. (1972) *J. Am. Chem. Soc.* **94,** 5612–5625.
11. Warshel, A. (1973) *Isr. J. Chem.* **11,** 709–717.
12. Warshel, A. (1977) in *Modern Theoretical Chemistry,* ed. Segal, G. (Plenum Publishing Co., New York), Vol. 7.
13. Warshel, A. & Levitt, M. (1974) *Quantum Chem. Program Exchange, No. 247,* Indiana University.
14. Warshel, A. (1977) *Annu. Rev. Biophys. Bioeng.* **6,** 273–300.
15. Warshel, A. & Karplus, M. (1974) *J. Am. Chem. Soc.* **96,** 5677–5680.
16. Fermi, G. (1975) *J. Mol. Biol.* **97,** 237–246.
17. Adams, D. M. (1968) *Metal-Ligand and Related Vibrations* (St. Martin's Press, New York).
18. Heidner, E. J., Ladner, R. C. & Perutz, M. F. (1976) *J. Mol. Biol.* **104,** 707–722.
19. Takano, T. (1977) *J. Mol. Biol.,* in press.
20. Sussner, H., Mager, A., Brunner, H. & Fasold, H. (1974) *Eur. J. Biochem.* **41,** 465–469.
21. Spiro, T. G. & Streakas, T. C. (1974) *J. Am. Chem. Soc.* **96,** 338–345.
22. Spaulding, L. D., Chang, C. C., Yu, Nai-Teng & Felton, R. H. (1974) *J. Am. Chem. Soc.* **97,** 2517–2525.
23. Brault, D. & Rougee, M. (1974) *Biochemistry* **13,** 4591–4597.
24. Brault, D. & Rougee, M. (1974) *Biochem. Biophys. Res. Commun.* **57,** 654–658.
25. Collman, J. P., Brauman, J. I. & Suslick, K. S. (1975) *J. Am. Chem. Soc.* **97,** 7185–7180.